

In Vivo Mechanical Characterization of the Distraction Callus During Bone Consolidation

J. MORA-MACÍAS,¹ E. REINA-ROMO,¹ M. LÓPEZ-PLIEGO,² M. A. GIRÁLDEZ-SÁNCHEZ,² and J. DOMÍNGUEZ¹

¹Department of Mechanical Engineering, Escuela Técnica Superior de Ingeniería, University of Seville, Camino de los Descubrimientos s/n, 41092 Seville, Spain; and ²Department of Orthopedics, Virgen del Rocío Hospital, 41013 Seville, Spain

(Received 6 February 2015; accepted 27 April 2015; published online 9 May 2015)

Associate Editor Peter E. McHugh oversaw the review of this article.

Abstract—Understanding the evolution of callus mechanical properties over time provides insights in the mechanobiology of fracture healing and tissue differentiation, can be used to validate numerical models, and informs clinical practice. Bone transport experiments were performed in sheep, in which a distractor type Ilizarov was implanted. The forces through the fixator evolution were measured and the callus stiffness was estimated from these forces. Computerized tomography images were taken and bone volume of the callus at different stages was obtained. The results showed that the maximum bone tissue production rate (0.146 cm³/day) was achieved 20 days after the end of the distraction phase. 50 days after the end of the distraction phase, the callus was ossified completely and had its maximum volume, 6–10 cm³. In addition, 80–90% of the load sustained by the operated limb was recovered and the callus stiffness increased exponentially until 5.4–11.4 kN/mm, still below 10% of the healthy level of callus stiffness. The effects of the bony bridging of the callus and the time of the fixator removal on callus force, stiffness and volume were analyzed. These outcomes allowed relating quantifiable biological aspects (callus volume and tissue production rate) with mechanical parameters (callus force and stiffness) using data from the same experiment.

Keywords—Callus volume, Stiffness monitoring, Force monitoring, Distraction osteogenesis, Bone transport, Bone tissue production rate.

INTRODUCTION

Distraction osteogenesis creates new bone tissue from an osteotomy by pulling away a bone segment

from the other.^{24,25} Bone transport is a specific type of distraction osteogenesis that is widely used for the treatment of long bone defects.^{7,10} The complete process of distraction osteogenesis consists of: an osteotomy of the bone; a latency phase, between performance of osteotomy and start of the traction, during which a soft callus is formed; a distraction phase, which allows the extension of the callus to the final desired length separating the two bone parts; a consolidation phase, during which the callus completes its formation and the tissue begins to organize as bone tissue; and finally, the bone remodeling of the callus.

Knowing the evolution of the callus biological and mechanical parameters over time is very important to understand the mechanobiology of the complete distraction osteogenesis process and optimize the application of this technique in clinical practice by means of the validation and later application of numerical models of distraction^{26,38–43} Currently, X-rays and manual clinical examinations are used commonly to estimate the status of the regenerative callus tissue in daily clinical routines. Nevertheless, both methods have been proven inexact.^{35,36,50} In addition, as these traditional techniques, many of the existing studies^{3,5,6,13,20,24,25,27,34} are not able to provide the sufficient quantitative information that sometimes may be necessary; e.g., to evaluate the time to remove the fixator. Therefore, new quantitative techniques for assessing callus volume and material properties are required to optimize clinical treatment strategies. Other *in vivo* and *ex vivo* experimental studies have evaluated quantitatively the callus mechanical properties or others mechanical parameters involved in the process of distraction osteogenesis and fracture healing. In previous experiments, *ex vivo* mechanical evaluation of the callus has used compression,^{19,33} bending,¹⁹ torsion,¹⁹ indentation^{28–30} or acoustic

Address correspondence to J. Mora-Macías, Department of Mechanical Engineering, Escuela Técnica Superior de Ingeniería, University of Seville, Camino de los Descubrimientos s/n, 41092 Seville, Spain. Electronic mail: juanmora@us.es, erreina@us.es, macarenalopezpliego@gmail.com, miguelgiraldez@yahoo.com, jaime@us.es

microscopy³⁷ tests to evaluate the mechanical properties of the callus. However, their results are limited since the environment, the boundary conditions and the applied loads in an *ex vivo* sample in the lab are not exactly the same as those within tissues *in vivo*. Moreover, the results of *ex vivo* mechanical tests are particular to the animal model and testing methods used making it difficult to compare studies; e.g. Rodríguez-Florez *et al.*,⁴⁶ demonstrated that it is not possible to compare mechanical properties obtained by indentation from studies using different preparation, testing and analysis methods.

Previous *in vivo* studies have used instrumented fixators to determine forces through the callus during the distraction phase^{4,7,21,49} or interfracture movement in the consolidation phase.¹⁰ *In vivo* models of fracture healing have measured forces through the callus during healing,^{18,22} which is similar to the consolidation phase of distraction osteogenesis. Nevertheless, as far as the authors know, the forces through the callus during the consolidation phase for distraction osteogenesis have not been previously evaluated.

Among the parameters to be measured to obtain the mechanical properties of the callus, the stiffness is the most frequently studied, and the one most capable of providing information about the process. The callus stiffness is defined as the force or torque applied to the callus divided by the displacement or angle induced, respectively. *In vivo* studies have assessed the stiffness of the callus and of the total affected limb both in distraction osteogenesis^{16,23,51} and fracture healing.^{9,12,23,45} They used different devices that allow measuring torsional,⁵¹ bending^{16,23,45} or axial^{2,9,12} stiffness of the callus, although these methods have some drawbacks. For instance, they do not measure the callus stiffness under real load conditions in patients, e.g., during gait. Instead, different external loads were applied manually: torsion of a bone segment respect to the other,⁵¹ bending of the intervened bone^{16,23,45} or compression.^{2,9,12} Some studies in literature used physiological conditions during gait but not in the measurement of the stiffness during fracture healing or distraction osteogenesis.^{11,15,48} Knowing the callus stiffness under real load motion conditions is useful for estimating the real load sustained by the callus because the callus presents a non-linear viscoelastic behavior.^{7,21} Additionally, the risk of bone misalignment exists in bending cases^{16,23,45} because segments have to rotate respect to each other during measurements, especially when the callus is not stiff enough. It means that, during some instants, the ideal alignment of segments of the long bone is not kept. It could affect the final alignment of the bone after the callus consolidation. Finally, most of these studies did not provide any calibration data for their respective devices.

As far as the authors know, most of the works referenced and others in literature focus on a single aspect of the process of distraction osteogenesis^{2,3,5-7,9,10,12,13,16,19,20,23-25,27,28,30,34,37,45,50,51} Therefore, the aim of this work is to quantify and relate during the complete bone transport process quantifiable biological parameters (the bone tissue volume and its distribution in the distraction callus) with mechanical parameters (the force through the fixator and through the callus, and the callus stiffness during the consolidation phase of the process). Bone transport experiments were performed in sheep. During the course of the process, a tested and calibrated device allowed measuring the forces and estimating the callus stiffness. The evolution of the state of the callus maturation was monitored *via* computed tomography (CT). Bone tissue volume of the callus was obtained from 3D reconstruction of the CT images.

MATERIALS AND METHODS

Instrumented Fixator for Force and Stiffness Measurements

For each animal, bone transport was applied using an instrumented Ilizarov type distractor^{31,32} (Fig. 1). The distractor was fixed to the proximal and distal bone segments of the distraction site. It was also attached to the bone transportable segment which is displaced 15 mm filling the distal defect and elongating the proximal distraction callus. The complete device to measure forces (fixator and acquisition systems) consisted of an instrumented fixator with six load cells in the bars, a force platform (OR6-7-1000, AMTI®, Watertown, Massachusetts, USA), two A/D converters for the load cells and the force platform, and a PC to record the data. The A/D converter of the load cells allowed transmitting the signals wirelessly from the animals (Fig. 2). The device allowed measuring the ground reaction force (GRF) with the force platform and the force through the fixator with the load cells.

Figure 1c shows a simplified scheme of the force distribution in an intervened limb during gait. The distraction callus was represented by a spring (K_a) as well as the docking site (K_b). On the other hand, the fixator proximal deformable elements were represented by K_{fi} and, the fixator distal deformable elements were represented by K_{fd} . The bone transportable segments were fixed to the fixator by means of Steinmann pins (K_h) which were considered non deformable compared to K_a and K_b during the distraction phase but very compliant compared to the docking site during the consolidation phase. The bone-fixator system is loaded with an internal force (IF). IF is the sum of GRF and

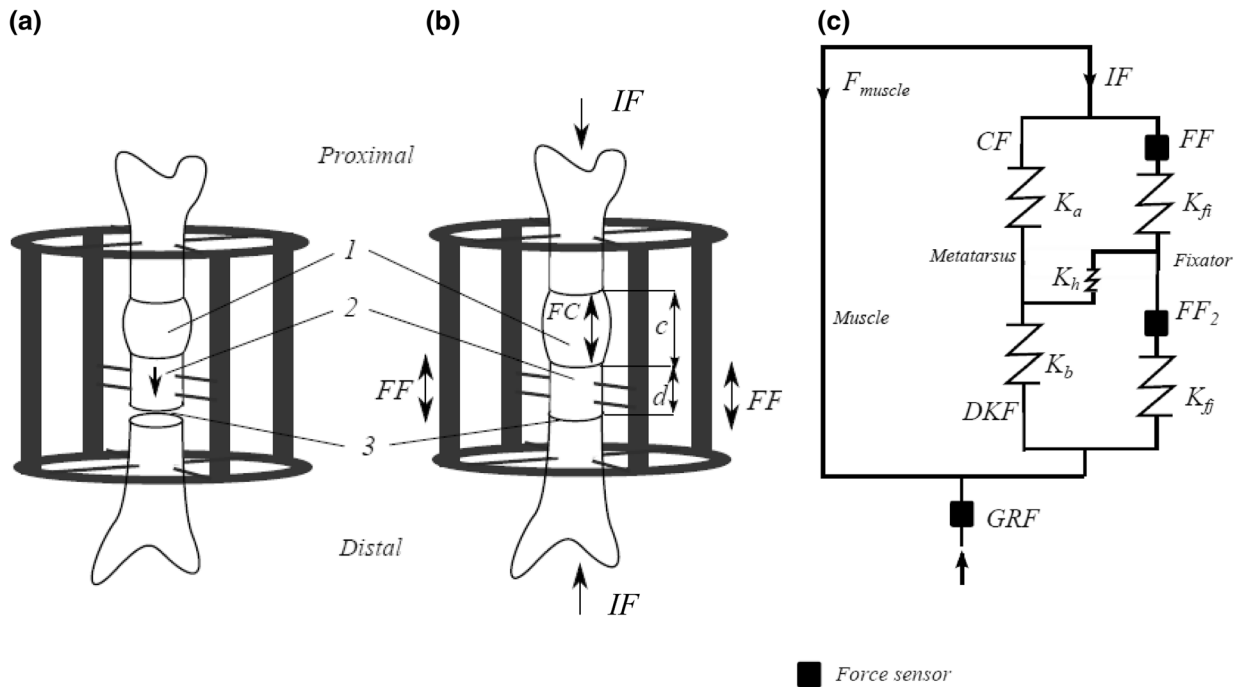


FIGURE 1. Scheme of the bone with the distractor³²: (a) during the distraction phase and (b) during the consolidation phase. (1) Distraction callus ($c = 15 \text{ mm}$); (2) bone transportable segment ($d = 25 \text{ mm}$); (3) docking site; FC force through the distraction callus; FF force through the fixator; and IF, force through the metatarsus or internal force. (c) Scheme of force distribution during gait in the limb where the fixator was implanted.

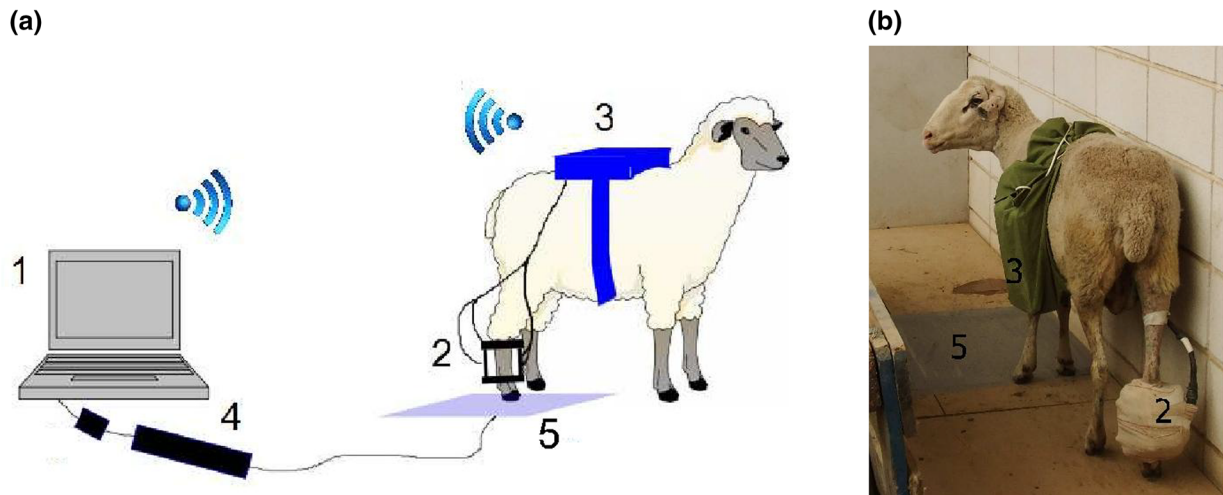


FIGURE 2. (a) Scheme of the acquisition system to measure forces³¹: (1) PC; (2) instrumented fixator with load cells; (3) A/D converter for the load cells signals; (4) A/D converter for the force platform signal; (5) force platform. (b) Sheep during a gait test.

the muscle activity over the bone (F_{muscle}). When IF is applied to the bone-fixator system, it is divided between force through the callus (CF) and force through the proximal part of the fixator (FF); or it is divided between force through the docking site (DKF) and force through the distal part of the fixator (FF_2). The used acquisition system allowed measuring FF, FF_2 , and GRF and the aim of this work was to obtain CF compared to FF and K_a .

According to this model $CF = IF - FF$. During the distraction phase, $K_b \approx 0$ and $DKF \approx 0$; therefore $IF \approx FF_2$ and CF could be obtained. In addition, the ratio IF/GRF was obtained every day during gait. It was observed that this ratio was approximately constant along the distraction phase. The mean value of IF/GRF measurements in all animals was 3.22 ± 0.46 , similar to values obtained in previous works.¹⁵ During the consolidation phase, $K_b \neq 0$ and IF could not be

measured directly. Authors assumed that the ratio IF/GRF during the consolidation phase was approximately constant and equal to the mean value measured during the distraction phase for each animal. This means that $F_{\text{muscle}}/\text{GRF}$ is assumed to be constant when the same physical activity is being performed (gait in this case). This assumption allowed estimating IF from GRF during the consolidation phase and, therefore, estimating CF.

A more sophisticated model of the used device was necessary to estimate K_a from force measurements and the stiffness of the different elements of the fixator which were evaluated experimentally. In addition, calibration experiments were performed *in vitro* where K_a was simulated with springs of known stiffnesses. This calibration process allowed taking into account the non-linear behavior of some elements of the fixator. It has been described in a previous work.³¹

Surgery

A standard surgery was performed for each animal using general anesthesia to implant the distractor. Three osteotomies were made, resulting in two small bone fragments. The distal bone fragment was retired, creating the defect, and the proximal, the bone transportable segment, was fixed to the distractor before cutting. Thus, there were two focus areas during the bone transport process: the distraction callus and the docking site (Fig. 1). The former, which is the aim of the study, represents the distance created by distracting the proximal osteotomy whilst the latter is the gap or the callus of union (depending on the phase, distraction or consolidation respectively) between the bone transportable segment and the most distal segment of the metatarsus (Fig. 1).

The fixator was applied to the metatarsal with the aid of an auxiliary tool for directing pins (Fig. 3). The auxiliary tool allows drilling the fixator's Schanz screws and the Steinmann pins in the correct direction. Therefore, the bone overloading due to correction of trajectory is avoided. This tool consists of two edges where two bearings can be moved and positioned at each point where a pin has to be drilled. Each bearing has guiding tubes to get an exact drilling trajectory. Before pins are drilled, the limb is fixed to the auxiliary tool's frame on proximal and distal ends and also in the middle one so that limb cannot move.

Animals and Protocol of Distraction

Eleven female Merino sheep, 3–5 years old, were used in this work. The body weight (BW) of the animals was 53.5 ± 8.5 kg. The welfare of the animals

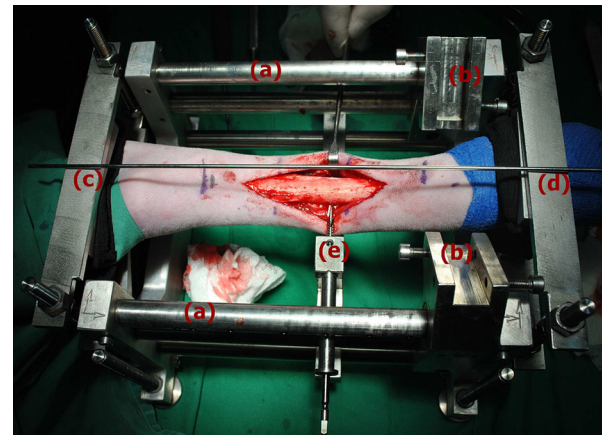


FIGURE 3. Auxiliary tool used during surgery: (a) edges; (b) bearings; (c–e) proximal, distal and middle limb fixation.

during the experiments was guaranteed by the experimentation ethics committee of the University of Seville.

First, the fixator was implanted surgically in the metatarsus of the right hind limb. After a latency period of a week, the distraction phase was carried out, moving the bone transportable segment 1 mm each day for 15 days to fill the defect, of 15 mm in length. After distraction, the consolidation phase was performed, until the distraction callus was ossified completely. Then, the distractor was removed, and bone remodeling continued. The time of the distractor removal was decided according to the force and stiffness measurements, to the X-ray controls and to the experience of the orthopedics surgeons and veterinarians that have collaborated in this experiment. The time of the distractor removal varied for each animal, being 153 ± 44 days from surgery. This variation was due to individual geometries of the bone and peculiarities of the callus maturation process for each sheep.

Measurement of Force and Stiffness

For each animal, gait tests were carried out three times per week during the distraction and consolidation phases. Each gait test (Fig. 2b) consisted of measuring GRF and FF. Afterwards, the rest of forces involved in the bone-fixator system while the sheep was walking as well as the callus stiffness were estimated as described in “Instrumented Fixator for Force and Stiffness Measurements” section. For a complete set of measurements, the animal had to tread at least 10 times with the intervened limb on the force platform. Mean forces of 5 valid treads were obtained. A tread was considered valid if the force data were measured when the sheep walked at 2–4 km/h.^{15,32}

CT Study and Measurements of the Callus Volume

CT images of the intervened limb were taken at different moments of the process to assess the state of maturation of the callus with time. The resolution of the CT images was 200–300 μm/voxel. The callus volume was obtained from CT images by segmentation, using the software *MIMICS*[®] (Materialise, Leuven, Belgium). In the segmentations carried out after the consolidation phase, it was not possible to differentiate automatically the bone tissue within the callus from the cortical bone tissue. In these cases, the limits of the callus were estimated manually. The total callus volume was quantified as well as the external and the internal callus volumes. External and internal volumes of the callus are defined according to Fig. 4.

CT images were performed both *in vivo* and *ex vivo*. CT images could not be performed *in vivo* in limbs which had the fixator installed due to the reflections of the metallic parts. To carry out CT images before callus was ossified completely, nine animals were sacrificed interrupting the process at different stages (17, 22, 29, 35, 37, 51, 79, 98, and 161 days after surgery). In these cases, to avoid misalignment of the bone segments, the distractor was removed only after the limb with the fixator from each sacrificed animal was frozen. The other two animals were studied after the callus had been totally ossified and the distractor had been removed. Hence, animals were not sacrificed and various CT images *in vivo* could be taken from each animal (137, 205, 277, 311, 379 and 471 days after surgery).

Statistical Analysis

The evolution of the fixator force and the callus force with time were correlated with the sum of two

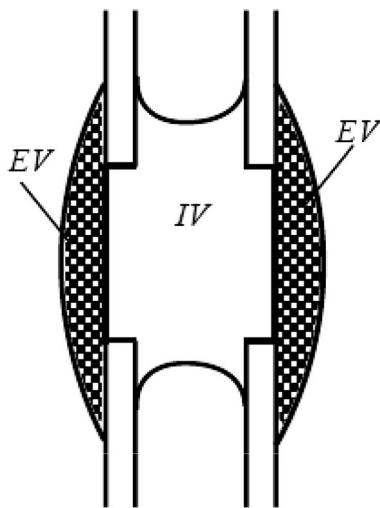


FIGURE 4. Section view of a callus: external volume of the callus (EV) and internal volume of the callus (IV).

logistic functions according to the trend observed in results below and in the literature^{2,22}:

$$XX = \frac{0.5 \cdot \overline{IF}}{1 + e^{a_{XX}(t+b_{XX})}} + \frac{0.5 \cdot \overline{IF}}{1 + e^{c_{XX}(t+d_{XX})}}, \quad (1)$$

where *XX* is FF or CF, \overline{IF} is the mean value of the internal force measured during the process, *t* is the time in days from surgery, a_{XX} , b_{XX} , c_{XX} and d_{XX} are the fitting coefficients.

The increase of the stiffness of the callus with time was modeled with a linearized exponential correlation according to the trend observed in results below and in the literature^{1,8,16,45}:

$$K = g e^{ht}, \quad (2)$$

where *K* is the callus stiffness, *t* is the time in days from surgery, *g* and *h* are the fitting coefficients.

Finally, the evolution of the total, external and internal volumes of the callus with time were correlated as the difference between two logistic functions:

$$ZZ = \frac{N_{ZZ}}{1 + e^{o_{ZZ}(t+q_{ZZ})}} - \frac{N_{ZZ} - M_{ZZ}}{1 + e^{r_{ZZ}(t+s_{ZZ})}}, \quad (3)$$

where *ZZ* is the total, external or internal volume of the callus, *t* is the time in days from surgery and o_{ZZ} , q_{ZZ} , r_{ZZ} , and s_{ZZ} are the fitting coefficients. N_{ZZ} is the maximum value of the total, external or internal volume of the callus during the process. Finally, M_{ZZ} is the value of the total, external or internal volume of the callus after bone remodeling, i.e., approximately the volume of the bone fragment extracted during surgery to create the gap for the total and the internal volume correlations and zero for the external volume correlation.

The significance of each correlation was estimated by means of a lack-of-fit test. Pearson correlation analyses were conducted to the linear correlation of the callus stiffness. In the non-linear regressions, it is not possible to construct an exact *F* test of size *p* (probability of no correlation); however, it is possible to determine an asymptotic value of *p* if the sample is reasonably large.⁴⁷ The regressions were considered significant if $p < 0.05$.

RESULTS

Callus-Fixator Force Distribution

Figure 5a shows the CF, the FF and the IF values for the gaits tests performed during the process and their correlations vs. time for CF and FF. The values were normalized to BW, to take into account BW differences between the animals. The mean value of IF (\overline{IF}) was calculated and is also represented, being

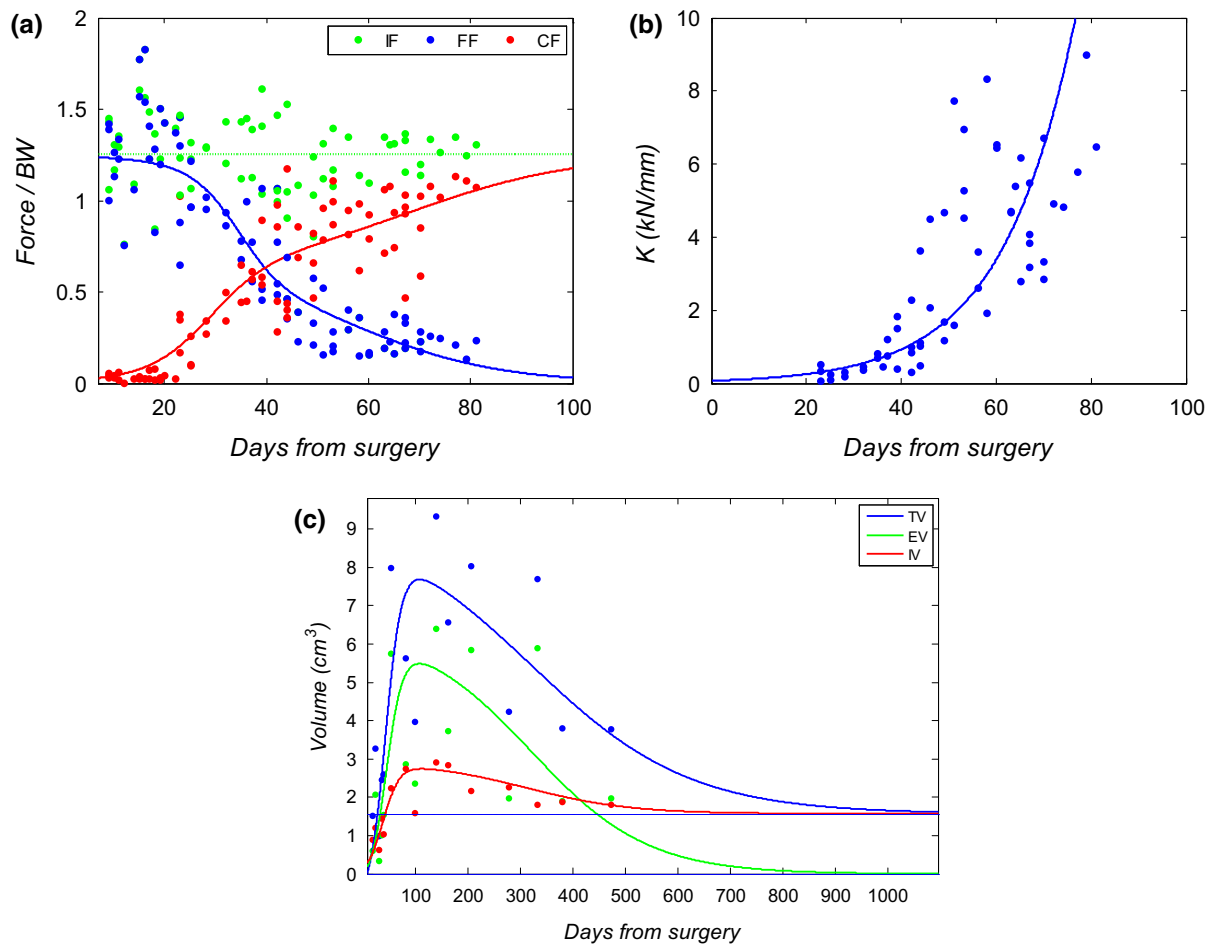


FIGURE 5. (a) Experimental force distribution during bone transport process normalized to BW (points): force through the fixator (FF), force through the callus (CF) and internal force (IF). The correlations for FF and CF (continuous lines) and the mean value for IF (dotted line) are also shown. (b) Evolution of the stiffness of the callus (K) during bone transport process. Experimental values (points) and correlation (continuous line) are shown. (c) Evolution of the total, the external and the internal bone volume of the callus until 3 year after surgery. Experimental values (points) and correlations (continuous line) are shown. The dotted line is approximately the volume of the bone fragment extracted during surgery to create the gap (M).

TABLE 1. Coefficients and statistical parameters of the fitting of fixator force (FF) and callus force (CF) vs. time from surgery normalized to BW.

	a_{xx}	b_{xx}	c_{xx}	d_{xx}	\bar{IF}	R^2	p
XX = FF	0.226	-34.408	0.070	-57.283	1.257	0.8153	<0.001
XX = CF	-0.170	-28.987	-0.062	-68.704	1.257	0.7788	<0.001

1.26 BW. It can be seen that CF increased from approximately 0.05–0.2 BW (3–12% of \bar{IF}), at the end of the distraction phase, to 0.8–1.2 BW 70 days after surgery approximately (80–90% of \bar{IF}). FF followed an opposite trend, it decreased from 0.9 to 1.2 BW (90–100% of \bar{IF}), to 0.1–0.3 BW 70 days after surgery approximately, (6–9% of \bar{IF}).

For the CF and FF correlations, Eq. (1) was used. Table 1 shows the coefficients and the calculated statistical parameters (i.e., the coefficient of determination,

R^2 , and the p values). Both correlations were significant according to the p values obtained.

Callus Stiffness

Figure 5b shows the estimated value of the callus stiffness after the distraction phase and its correlation with time. At the end of the distraction phase the callus stiffness was approximately 0.13–0.27 kN/mm. During the consolidation phase, the callus stiffness increased

exponentially reaching 5.4–11.4 kN/mm in 50 days of consolidation (70 days from surgery), i.e. the callus stiffness increased an average of 40 times in 7 weeks.

The coefficients of the exponential linearized regression used (Eq. (2)) and the calculated statistical parameters are reported in Table 2. The correlation was significant.

TABLE 2. Coefficients and statistical parameters of the fitting of the callus stiffness vs. time from surgery.

g	h	R^2	p
68.947	0.064	0.713	<0.001

Volume and Distribution of the Bone Tissue of the Callus

Section views of the callus with time from CT images are shown in Fig. 6. It can be seen that the bone tissue appeared in the callus during the distraction phase close to the bone segments that limit the callus and the periosteum. The bony bridging of the callus took place one or two weeks after the end of the distraction phase (29–35 days after surgery). It happened in the external callus firstly according to the callus section views of days 22, 29 and 37 (Fig. 6). During the consolidation phase, it can be seen how the callus grew internally and externally, achieving the maximum callus volume and exterior diameter about 90–150 days

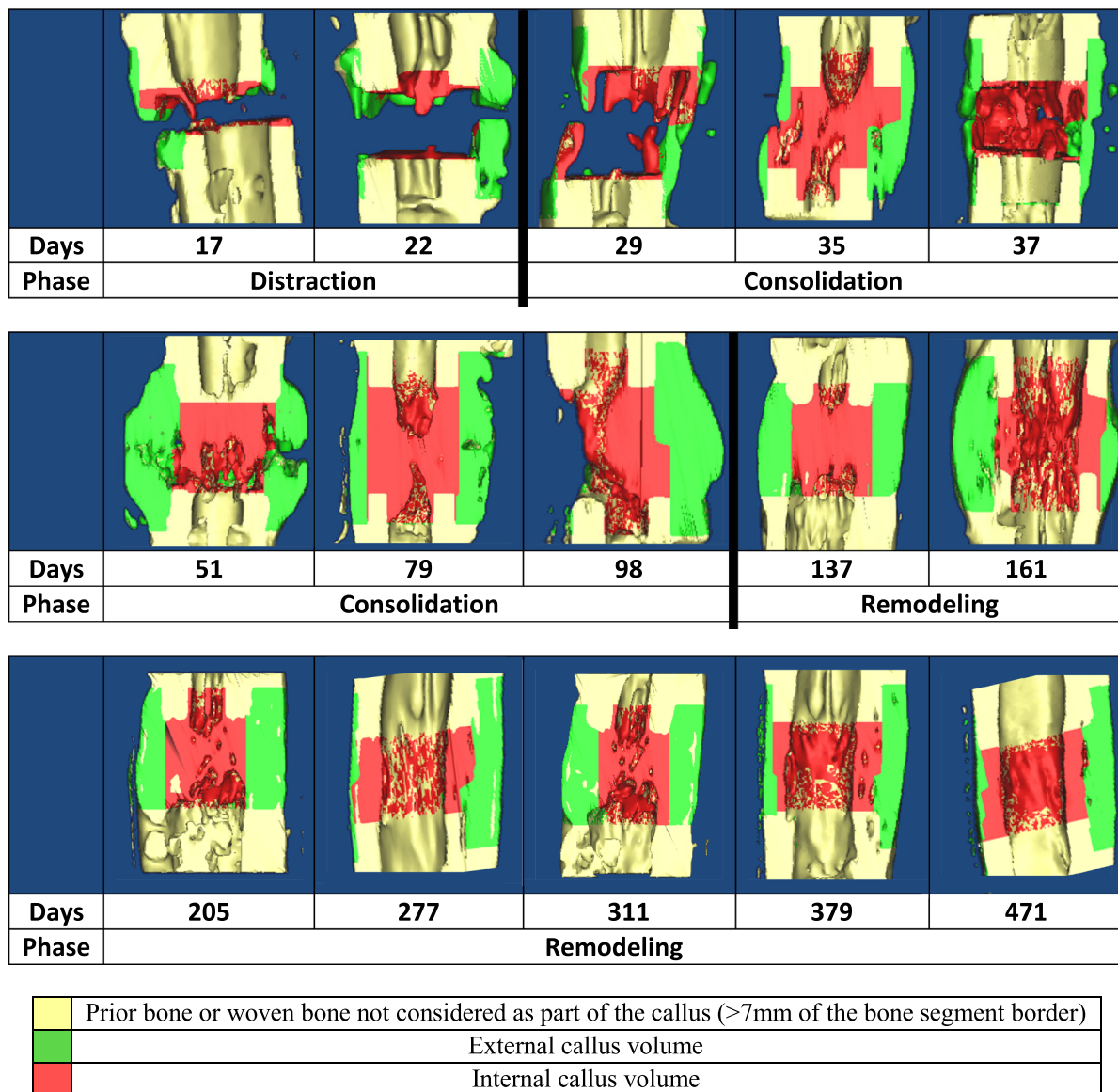


FIGURE 6. Callus section views in different days after bone transport surgery.

after surgery. The callus section views from day 137 shows the medullar canal formation and the slowly reduction of the external diameter of the callus.

Figure 5c shows the value of total, external and internal bone tissue volumes of the callus with time estimated from the different CT images. The correlations for these values with time are also shown. These correlations of the total, external and internal bone tissue volume evolution with time are in concordance with callus section views of Fig. 6. The total callus volume increased from zero at the beginning of the process to a maximum of 6–10 cm³ approximately 90–150 days after surgery. After the maximum volume was achieved, it can be observed how the bone recovered its original shape after approximately 1 year (See Figs. 5c, 6). The external and internal volumes of the callus had a trend close to the total volume trend, with maximum values of 4–6 and 2–3 cm³ respectively (Fig. 5c) for 90–150 days after surgery. After the peak, the external volume decreased to zero and the internal volume decreased to approximately the volume of the bone fragment extracted during surgery to create the gap. The external volume was greater than the internal until 380–420 days after surgery. After this time, the bone loss was more significant in the external volume.

Significant correlations were obtained for the total and the external volumes of the callus with two logistic functions (Eq. (3)). The coefficients and the calculated statistical parameters are shown in Table 3.

The bone tissue production rate may be calculated as the derivative of the total callus bone volume correlation (Eq. (3)). The maximum bone tissue production rate was 0.146 cm³/day. It was achieved approximately 40 days after surgery.

DISCUSSION

This experimental work evaluated the force through the callus as well as the axial stiffness of the callus during the bone transport process, from directly measurements of the ground reaction force and the force through the fixator. The evolution of these mechanical parameters was compared with the level of ossification of the callus quantified by the volume of the bone tissue and bone tissue production rate with time. To the best of our knowledge, few studies have related the

mechanical parameters evolution with quantifiable biological aspects of the complete process of distraction osteogenesis. Moreover, the information of the results of these experiments is useful in daily clinical routines to understand the mechanobiology of the process and to validate numerical models of distraction.

As far as the authors know, there are no works where force evolution has been monitored during the consolidation phase of the distraction osteogenesis process in sheep. However, there are some works in the literature, which can be used as reference for comparison of data force. Duda *et al.*¹⁵ calculated the maximum internal force in metatarsus of sheep during walking in fracture healing. In hind limbs it was 1–1.3 BW approximately, close to the values of \overline{IF} in this work, 1.26 BW. On the other hand, according to the force data (Fig. 5a), the intervened limb recovered its capacity of sustaining the gait force ($CF \approx 80\text{--}90\%$ of the \overline{IF}) after 50 days of consolidation, i.e. 70 days from surgery. Other works in literature report that 80–90% of the total force sustained by the limb was recovered: after approximately 30 days of consolidation for fracture healing in sheep²²; after approximately 50 days of consolidation for fracture healing in rabbits¹⁸; after approximately 100 days of consolidation for fracture healing in human tibias⁹; and after approximately 200 days of consolidation for distraction osteogenesis (with an average bone lengthening of 31 mm) in human tibias.²

The callus stiffness can be related to an average elastic modulus of the callus assuming a cylindrical geometry of the callus (average length 12.7 mm, average diameter 14.93 mm) and homogeneous material properties. During the consolidation phase, the callus stiffness increased exponentially from 0.13–0.27 to 5.4–11.4 kN/mm (Fig. 5b), or equivalently, the average elastic modulus of the callus increased from 10.5–21.8 to 436.6–921.7 MPa approximately. Although, the estimation of the average elastic modulus implies some assumptions, it could be interesting to note that these results are in the same order of magnitude than those obtained by Leong and Morgan.^{28,29} They evaluated the elastic modulus of the bone tissue of the callus in fracture healing by means of nanoindentation. Values obtained for the elastic modulus of the bone tissue of the callus were 27–1010 MPa approximately. On the other hand, an exponential increase of callus stiffness

TABLE 3. Coefficients and statistical parameters of the fitting of the total (TV), external (EV) and internal (IV) volumes of the callus vs. time from surgery.

	o_{zz}	q_{zz}	r_{zz}	s_{zz}	N_{zz}	M_{zz}	R^2	P
ZZ = TV	−0.065	−42.000	−0.007	−320.000	9.346	1.572	0.484	0.002
ZZ = EV	−0.065	−44.025	−0.009	−320.004	6.415	0.000	0.325	0.017
ZZ = IV	−0.065	−37.783	−0.010	−310.000	2.931	1.572	0.115	0.289

was shown in other works such as Dwyer *et al.*,¹⁶ for experiments of distraction osteogenesis in human tibias.

The evolution of the total bone volume of the callus marked the different biological stages of the process (Figs. 5c, 6). During the distraction phase the activity of ossification started near the periosteum and the bony bridging of the callus took place a week after the end of this phase (Fig. 6). These facts could be observed in radiographies or CT images in other works^{27,33,44} and showed the important role that the periosteum membrane has during distraction osteogenesis.^{14,52} During the consolidation phase, the period of maximum ossification took place from 20–70 days after surgery (Fig. 5c). The distribution of the bone tissue volume of the callus (Figs. 5c) showed that the external or periosteal volume of the callus was more than 50% of the total volume during the consolidation phase. This increase in diameter around the callus was appreciable in radiographies, histologies or CT images provided by other works in distraction osteogenesis.^{27,39,44} The peak of callus volume time (90–150 days after surgery) coincided approximately with the distractor removal (109–197 days after surgery). This was a suitable time to retire the distractor, since the limb had recovered its capacity to sustain internal forces and the callus stiffness had increased enough (Figs. 5a, and 5b). Furthermore, a study with the same distraction protocol in sheep,³² reported that at this moment (150–200 days from surgery approximately), the animals almost recovered their normal gait conditions, after the lameness induced by the surgery. After distractor removal, total external and internal volumes decreased due to bone remodeling.

As far as the authors know no studies in literature allow comparing mechanical parameters with biological aspects of the distraction osteogenesis process. Figure 7 relates these parameters; it shows the callus force (a), the total bone tissue volume (b) and the bone tissue production rate (c) vs. the callus stiffness during 80 days after surgery. During the period of maximum ossification (20 to 70 days after surgery), maximum bone tissue production rate was achieved (Fig. 7c) and total, external and internal volumes increased from zero to 80% of their maximum values (Fig. 7b). This period also coincided with the recovery of load sustained by the intervened limb (from 3 to 12% of \bar{IF} to 60–70% of \bar{IF} , Fig. 7a). However, this period of maximum ossification corresponded to low callus stiffness, which increased from approximately zero to 2–3% of the stiffness of a healthy segment of a metatarsus with the same length. According to Figs. 7a and 7b, 90% of the maximum total, internal and external volumes of the callus were achieved and 80% of the IF loaded the callus when callus stiffness was under

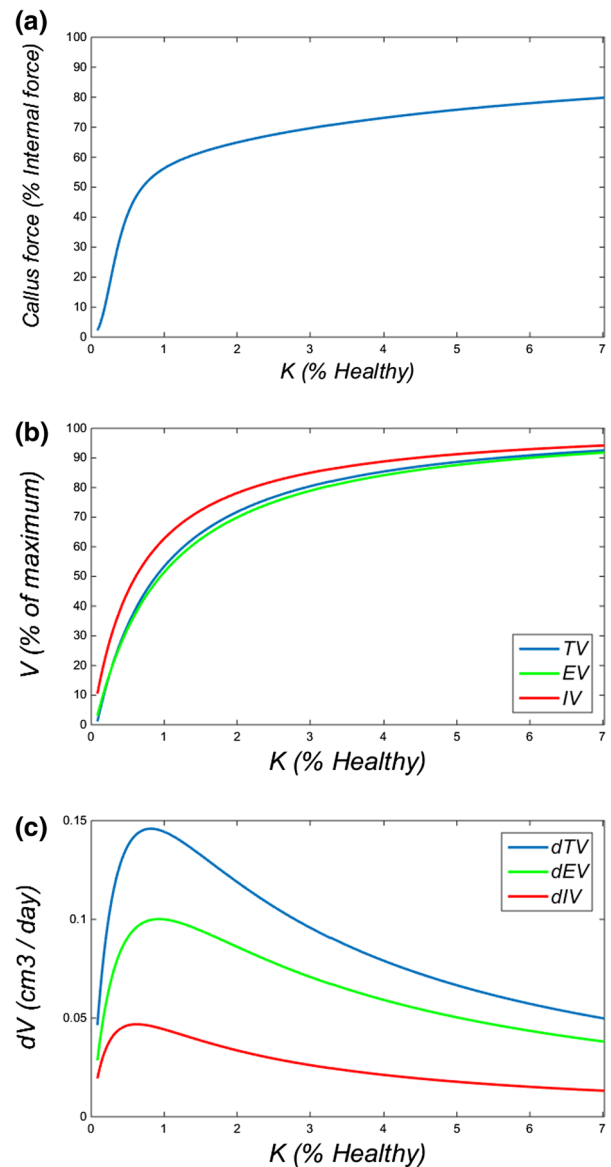


FIGURE 7. (a) Callus force normalized to \bar{IF} , (b) total, external and internal bone tissue volume normalized to maximum values and (c) bone tissue production rate vs. callus stiffness normalized to the stiffness of a healthy segment of the metatarsus with the same length (assuming 15 and 9 mm of external and internal diameter respectively and an elastic modulus of 17 GPa¹⁷).

10% of the stiffness of a healthy segment of a metatarsus with the same length. Therefore, it can be concluded that callus volume is a good indicator of the load bearing capacity of the intervened limb but not of the stiffness. It means that usual examinations by means of radiographies may predict the load bearing capacity but not the recovery of stiffness of the intervened limb. It is expected that the higher stiffness increase takes place after maximum callus volume is achieved and once load bearing capability is recovered, i.e. during the bone remodeling phase. During bone

remodeling it is expected that bone tissue reorganizes and elastic modulus of the new bone increases, resulting in an increase of callus stiffness until asymptotic healthy value. However, during the consolidation phase, bone volume is created quickly in a disorganized way with the aim of recovering the force sustained by the limb.^{20,24,25,44}

The device (instrumented fixator and acquisition system; Fig. 2) used in this study or similar designs increase the future possibilities of assessing consolidation in combination with conventional methods (such as X-rays or *ex vivo* tests). In addition, it presented some advantages³¹ over conventional methods and others devices in the literature to assess the stiffness by means of force monitoring^{2,9,12,16,23,45,51}: it allows measuring force and stiffness under real load motion conditions, without a risk of bone axial transverse misalignment, measurements are non-invasive, beyond the fixator implantation, and it does not expose the patient to radiation.

Although the outcomes in stiffness evaluation shown are rewarding, there are some limitations associated to the methods employed to measure force and stiffness. On the one hand, the noise in force signals caused an error of ± 1 N approximately. In addition, the range of stiffness measurement is limited from 1 to 10,000 N/mm.³¹ On the other hand, it could be observed interindividuals differences in the shape of the callus with time. For example the appearance of the medular canal happened with a difference of ± 50 days depending on each animal (Fig. 6, 161–379 days).

The findings of this study might help to understand the mechanobiology of the process of distraction osteogenesis and to complement previous experimental and computational works. The outcomes combine information about the evolution of force and stiffness in the distraction callus, the level of ossification shown by CT images and the volume of bone tissue within the callus. Furthermore, the used method could be applied, with the adequate adaptations and developments, in cases of simple distraction or fracture healing during clinical daily routine. The force and stiffness data together with conventional methods such as radiographies may provide useful information about the evolution of the patients. For example, it allows knowing exactly when the limb stiffness is recovered while the fixator is implanted, or estimating the optimum time when the fixator should be retired.

ACKNOWLEDGMENTS

The authors gratefully acknowledge the research support of the Consejería de Innovación, Ciencia y Empleo de la Junta de Andalucía (P09-TEP-5195) and

the FPU grant of the Ministerio de Educación del Gobierno de España (AP2010-5061). The authors are also grateful to the University of Zaragoza for its collaboration.

CONFLICT OF INTEREST

The authors have no financial or personal relationships that could inappropriately influence the contents of this paper.

REFERENCES

- ¹Aarnes, G. T., H. Steen, L. P. Kristiansen, E. Festø, and P. Ludvigsen. Optimum loading mode for axial stiffness testing in limb lengthening. *J. Orthop. Res.* 24:348–354, 2006.
- ²Aarnes, G. T., H. Steen, P. Ludvigsen, N. A. Waanders, R. Huiskes, and S. A. Goldstein. In vivo assessment of regenerate axial stiffness in distraction osteogenesis. *J. Orthop. Res.* 23:494–498, 2005.
- ³Aronson, J. Temporal and spatial increases in blood flow during distraction osteogenesis. *Clin. Orthop. Relat. Res.* 301:124–131, 1994.
- ⁴Aronson, J., and J. H. Harp. Mechanical forces as predictors of healing during tibial lengthening by distraction osteogenesis. *Clin. Orthop. Relat. Res.* 301:73–79, 1994.
- ⁵Aronson, J., B. H. Harrison, C. L. Stewart, and J. H. Harp, Jr. The histology of distraction osteogenesis using different external fixators. *Clin. Orthop. Relat. Res.* 241:106–116, 1989.
- ⁶Aronson, J., X. C. Shen, R. A. Skinner, W. R. Hogue, T. M. Badger, and C. K. Lumpkin, Jr. Rat model of distraction osteogenesis. *J. Orthop. Res.* 15:221–226, 1997.
- ⁷Brunner, U. H., J. Cordey, L. Schweiberer, and S. M. Perren. Force required for bone segment transport in the treatment of large bone defects using medullary nail fixation. *Clin. Orthop. Relat. Res.* 301:147–155, 1994.
- ⁸Claes, L. E., and J. L. Cunningham. Monitoring the mechanical properties of healing bone. *Clin. Orthop. Relat. Res.* 467:1964–1971, 2009.
- ⁹Claes, L., R. Grass, T. Schmickal, B. Kisse, C. Eggers, H. Gerngross, W. Mutschler, M. Arand, T. Wintermeyer, and A. Wentzensen. Monitoring and healing analysis of 100 tibial shaft fractures. *Langenbecks. Arch. Surg.* 387:146–152, 2002.
- ¹⁰Claes, L., J. Laule, K. Wenger, G. Suger, U. Liener, and L. Kinzl. The influence of stiffness of the fixator on maturation of callus after segmental transport. *J. Bone Jt. Surg. Br.* 82:142–148, 2000.
- ¹¹Claes, L. E., H.-J. Wilke, P. Augat, S. Rübenacker, and K. J. Margevicius. Effect of dynamization on gap healing of diaphyseal fractures under external fixation. *Clin. Biomech. (Bristol, Avon)*. 10:227–234, 1995.
- ¹²Cunningham, J. L., J. Kenwright, and C. J. Kershaw. Biomechanical measurement of fracture healing. *J. Med. Eng. Technol.* 14:92–101, 1990.
- ¹³De Pablos Jr, J., and J. Canadell. Experimental physeal distraction in immature sheep. *Clin. Orthop. Relat. Res.* 250:73–80, 1990.

- ¹⁴Delloye, C., G. Delefortrie, L. Coutelier, and A. Vincent. Bone regenerate formation in cortical bone during distraction lengthening. An experimental study. *Clin. Orthop. Relat. Res.* 250:34–42, 1990.
- ¹⁵Duda, G. N., K. Eckert-Hubner, R. Sokiranski, A. Kreutner, R. Miller, and L. Claes. Analysis of inter-fragmentary movement as a function of musculoskeletal loading conditions in sheep. *J. Biomech.* 31:201–210, 1998.
- ¹⁶Dwyer, J. S., P. J. Owen, G. A. Evans, J. H. Kuiper, and J. B. Richardson. Stiffness measurements to assess healing during leg lengthening. A preliminary report. *J. Bone Jt. Surg. Br.* 78:286–289, 1996.
- ¹⁷Evans, F. G. *Mechanical Properties of Bone*. Springfield: Charles C. Thomas Publisher, 1973.
- ¹⁸Floerkemeier, T., W. Aljuneidi, J. Reifenrath, N. Angrisani, D. Rittershaus, D. Gottschalk, S. Besdo, A. Meyer-Lindenberg, H. Windhagen, and F. Thorey. Telemetric in vivo measurement of compressive forces during consolidation in a rabbit model. *Technol. Health Care* 19:173–183, 2011.
- ¹⁹Floerkemeier, T., F. Thorey, C. Hurschler, M. Wellmann, F. Witte, and H. Windhagen. Stiffness of callus tissue during distraction osteogenesis. *Orthop. Traumatol. Surg. Res.* 96:155–160, 2010.
- ²⁰Forriol, F., L. Denaro, U. G. Longo, H. Taira, N. Maffulli, and V. Denaro. Bone lengthening osteogenesis, a combination of intramembranous and endochondral ossification: an experimental study in sheep. *Strateg. Trauma Limb Reconstr.* 5:71–78, 2010.
- ²¹Gardner, T. N., M. Evans, H. Simpson, and J. Kenwright. Force-displacement behaviour of biological tissue during distraction osteogenesis. *Med. Eng. Phys.* 20:708–715, 1998.
- ²²Grasa, J., M. J. Gomez-Benito, L. A. Gonzalez-Torres, D. Asiain, F. Quero, and J. M. Garcia-Aznar. Monitoring in vivo load transmission through an external fixator. *Ann. Biomed. Eng.* 38:605–612, 2010.
- ²³Hente, R., J. Cordey, and S. M. Perren. In vivo measurement of bending stiffness in fracture healing. *Biomed. Eng. Online* 2:8, 2003.
- ²⁴Ilizarov, G. A. The tension-stress effect on the genesis and growth of tissues. Part I. The influence of stability of fixation and soft-tissue preservation. *Clin. Orthop. Relat. Res.* 238:249–281, 1989.
- ²⁵Ilizarov, G. A. The tension-stress effect on the genesis and growth of tissues: Part II. The influence of the rate and frequency of distraction. *Clin. Orthop. Relat. Res.* 239:263–285, 1989.
- ²⁶Isaksson, H., O. Comas, C. C. van Donkelaar, J. Mediavilla, W. Wilson, R. Huiskes, and K. Ito. Bone regeneration during distraction osteogenesis: mechano-regulation by shear strain and fluid velocity. *J. Biomech.* 40:2002–2011, 2007.
- ²⁷Kojimoto, H., N. Yasui, T. Goto, S. Matsuda, and Y. Shimomura. Bone lengthening in rabbits by callus distraction. The role of periosteum and endosteum. *J. Bone Jt. Surg. Br.* 70:543–549, 1988.
- ²⁸Leong, P. L., and E. F. Morgan. Measurement of fracture callus material properties via nanoindentation. *Acta Biomater.* 4:1569–1575, 2008.
- ²⁹Leong, P. L., and E. F. Morgan. Correlations between indentation modulus and mineral density in bone-fracture calluses. *Integr. Comp. Biol.* 49:59–68, 2009.
- ³⁰Manjubala, I., Y. Liu, D. R. Epari, P. Roschger, H. Schell, P. Fratzl, and G. N. Duda. Spatial and temporal variations of mechanical properties and mineral content of the external callus during bone healing. *Bone* 45:185–192, 2009.
- ³¹Mora-Macias, J., E. Reina-Romo, and J. Dominguez. Distraction device to estimate the axial stiffness of the callus in vivo. *Med. Eng. Phys.*, 2015 (Under review).
- ³²Mora-Macias, J., E. Reina-Romo, J. Morgaz, and J. Dominguez. In vivo gait analysis during bone transport. *Ann. Biomed. Eng.* 2015. doi:10.1007/s10439-015-1262-2.
- ³³Ohyama, M., Y. Miyasaka, M. Sakurai, A. T. Yokobori, Jr., and S. Sasaki. The mechanical behavior and morphological structure of callus in experimental callotaxis. *Biomed. Mater. Eng.* 4:273–281, 1994.
- ³⁴Okazaki, H., T. Kurokawa, K. Nakamura, T. Matsushita, K. Mamada, and H. Kawaguchi. Stimulation of bone formation by recombinant fibroblast growth factor-2 in callotaxis bone lengthening of rabbits. *Calcif. Tissue Int.* 64:542–546, 1999.
- ³⁵Panjabi, M. M., R. W. Lindsey, S. D. Walter, and A. A. White, 3rd. The clinician's ability to evaluate the strength of healing fractures from plain radiographs. *J. Orthop. Trauma* 3:29–32, 1989.
- ³⁶Panjabi, M. M., S. D. Walter, M. Karuda, A. A. White, and J. P. Lawson. Correlations of radiographic analysis of healing fractures with strength: a statistical analysis of experimental osteotomies. *J. Orthop. Res.* 3:212–218, 1985.
- ³⁷Preininger, B., S. Checa, F. L. Molnar, P. Fratzl, G. N. Duda, and K. Raum. Spatial-temporal mapping of bone structural and elastic properties in a sheep model following osteotomy. *Ultrasound Med. Biol.* 37:474–483, 2011.
- ³⁸Reina-Romo, E., M. J. Gomez-Benito, J. Dominguez, and J. M. Garcia-Aznar. A lattice-based approach to model distraction osteogenesis. *J. Biomech.* 45:2736–2742, 2012.
- ³⁹Reina-Romo, E., M. J. Gomez-Benito, J. Dominguez, F. Niemeyer, T. Wehner, U. Simon, and L. E. Claes. Effect of the fixator stiffness on the young regenerate bone after bone transport: computational approach. *J. Biomech.* 44:917–923, 2011.
- ⁴⁰Reina-Romo, E., M. J. Gomez-Benito, J. M. Garcia-Aznar, J. Dominguez, and M. Doblare. Modeling distraction osteogenesis: analysis of the distraction rate. *Biomech. Model. Mechanobiol.* 8:323–335, 2009.
- ⁴¹Reina-Romo, E., M. J. Gomez-Benito, J. M. Garcia-Aznar, J. Dominguez, and M. Doblare. Growth mixture model of distraction osteogenesis: effect of pre-traction stresses. *Biomech. Model. Mechanobiol.* 9:103–115, 2010.
- ⁴²Reina-Romo, E., M. J. Gomez-Benito, J. M. Garcia-Aznar, J. Dominguez, and M. Doblare. An interspecies computational study on limb lengthening. *Proc. Inst. Mech. Eng. H* 224:1245–1256, 2010.
- ⁴³Reina-Romo, E., M. J. Gomez-Benito, A. Sampietro-Fuentes, J. Dominguez, and J. M. Garcia-Aznar. Three-dimensional simulation of mandibular distraction osteogenesis: mechanobiological analysis. *Ann. Biomed. Eng.* 39:35–43, 2011.
- ⁴⁴Richards, M., J. A. Goulet, M. B. Schaffler, and S. A. Goldstein. Temporal and spatial characterization of regenerate bone in the lengthened rabbit tibia. *J. Bone Miner. Res.* 14:1978–1986, 1999.
- ⁴⁵Richardson, J. B., J. L. Cunningham, A. E. Goodship, B. T. O'Connor, and J. Kenwright. Measuring stiffness can define healing of tibial fractures. *J. Bone Jt. Surg. Br.* 76:389–394, 1994.
- ⁴⁶Rodriguez-Florez, N., M. L. Oyen, and S. J. Shefelbine. Insight into differences in nanoindentation properties of bone. *J. Mech. Behav. Biomed. Mater.* 18:90–99, 2013.

- ⁴⁷Ryan, T. P. *Modern Regression Methods*. Hoboken, NJ: Wiley, 2009.
- ⁴⁸Simon, U., P. Augat, A. Ignatius, and L. Claes. Influence of the stiffness of bone defect implants on the mechanical conditions at the interface—a finite element analysis with contact. *J. Biomech.* 36:1079–1086, 2003.
- ⁴⁹Waanders, N. A., M. Richards, H. Steen, J. L. Kuhn, S. A. Goldstein, and J. A. Goulet. Evaluation of the mechanical environment during distraction osteogenesis. *Clin. Orthop. Relat. Res.* 349:225–234, 1998.
- ⁵⁰Webb, J., G. Herling, T. Gardner, J. Kenwright, and A. H. Simpson. Manual assessment of fracture stiffness. *Injury* 27:319–320, 1996.
- ⁵¹Windhagen, H., S. Kolbeck, H. Bail, A. Schmeling, and M. Raschke. Quantitative assessment of in vivo bone regeneration consolidation in distraction osteogenesis. *J. Orthop. Res.* 18:912–919, 2000.
- ⁵²Yasui, N., H. Kojimoto, H. Shimizu, and Y. Shimomura. The effect of distraction upon bone, muscle, and periosteum. *Orthop. Clin. North Am.* 22:563–567, 1991.